Pöhlitz, J., Rücknagel, J., Koblenz, B., **Schlüter, S.**, **Vogel, H.-J.**, Christen, O. (2018):
Computed tomography and soil physical measurements of compaction behaviour under strip tillage, mulch tillage and no tillage
Soil Tillage Res. **175** , 205 – 216

Computed tomography and soil physical measurements of compaction behaviour under strip tillage, mulch tillage and no tillage

Julia Pöhlitz[1*], Jan Rücknagel[1], Barbara Koblenz[1], Steffen Schlüter[2], Hans-Jörg Vogel[2], Olaf Christen[1]

[1] Martin Luther University Halle-Wittenberg, Department of Agronomy and Organic Farming Betty-Heimann-Str. 5, 06120 Halle/Saale, Germany

[2] Helmholtz Centre for Environmental Research GmbH – UFZ, Department of Soil Physics, Theodor-Lieser-Str. 4, 06120 Halle/Saale, Germany

[*]Corresponding author: Email address: julia.poehlitz@landw.uni-halle.de, phone: 0049/3455522631, address: Department of Agronomy and Organic Farming, Martin Luther University Halle-Wittenberg, Betty-Heimann-Str. 5, 06120 Halle/Saale

Abstract

In recent years, there has been an increased application of conservation-oriented tillage techniques, where instead of being turned the soil is only loosened or not tilled at all. Strip tillage, a special form of conservation tillage, results in small-scale structural differences, since tillage is performed only within the seed row, while the soil between seed rows is not tilled. However, tillage always impacts upon physical soil properties and processes.

A combined application of conventional soil mechanical methods and X-ray computed tomography (X-ray CT) is employed here in order to investigate small-scale structural differences in a chernozem (texture 0-30 cm: silt loam) located in central Germany under strip tillage (within and between seed rows) compared to no tillage and mulch tillage. Apart from recording changes over time (years: 2012, 2014, 2015) to dry bulk density and saturated conductivity at soil depths 2–8 and 12–18 cm, stress-strain tests were conducted to map mechanical behaviour for a load range of 5–550 kPa at a soil depth of 12–18 cm (year 2015). Mechanical precompression stress was determined from the stress-dry bulk density curves. In addition, computed tomography scans were created followed by quantitative image analysis of the morphometric parameters mean macropore diameter, macroporosity, connectivity and anisotropy of the same soil samples.

For strip tillage between seed rows and no tillage, a significant increase in dry bulk density was observed over time compared to strip tillage within the seed row and mulch tillage. This was more pronounced at a soil depth of 2–8 cm than at 12–18 cm. Despite higher dry bulk density, strip tillage between the seed row displayed also an increasing saturated conductivity compared to strip tillage within the seed row and mulch tillage. The computed tomography scans showed that the macropores became more compressed and soil aggregates were pushed together as mechanical stress

increased, with the aggregate arrangement being transformed down into a coherent soil mass. The soil mechanical and morphometric parameters supported each other in terms of what they revealed about the mechanical properties of the soil structures. For instance, in the strip tillage between seed rows and no tillage treatments, the lack of soil tillage not only resulted in higher dry bulk densities, but also higher aggregate densities, mechanical precompression stress values, mean macropore diameters as well as lower macroporosity and connectivity values compared to mulch tillage and strip tillage within the seed row. The computed tomography parameters are therefore highly suitable for providing supplementary information about the compaction process. Overall, this study showed that strip tillage combines the advantages of no tillage and a deeper, soil conservation-oriented primary tillage because, on a small scale, it creates two distinct soil structures which are beneficial in terms of optimal plant growth as well as mechanical resistance by driving over the soil.

Keywords: pre-compression stress; dry bulk density; aggregate density; image analysis; soil compaction

1. Introduction

Soil tillage aims to increase crop yields and at the same time preserve ecological soil functions, like habitat functions and regulatory functions for water and nutrients. In recent decades, an increasing number of practitioners have abandoned traditional tillage methods which turn the soil using a plough (conventional) in favour of conservation-oriented soil tillage (see e.g. Licht and Al-Kaisi, 2005; Nowatzki et al., 2009). The latter does not involve turning the soil with a plough, but instead only loosening it or leaving it completely untilled. Conservation tillage thus covers the soil surface with dead plant material (Gajiri et al., 1999). This has both ecological and economic benefits for the soil, such as for example conserving water, preventing soil erosion, preserving economic productivity, reduced investments in machinery and less time spent on seedbed preparation (Carter, 2004; FAO, 1993). There are a variety of conservation tillage systems, which can be roughly divided into no tillage, mulch tillage, strip tillage, ridge tillage and minimum tillage (FAO, 1993). Strip tillage is special in that the soil is divided into a sowing zone and a soil management zone. The sowing zone, which is 5–15 cm wide, is worked mechanically down to a depth of 25 cm in order to optimise the soil and microclimate conditions for crop germination and growth, while the soil management zone is left untilled (Lal, 1983). Strip tillage therefore combines the conventional advantages of no tillage and those of deeper, non-turning primary tillage. It also allows farmers to combine individual working steps, thus reducing the number of times the field is driven over (Nowatzki et al., 2009).

However, any type of tillage affects the physical properties of the soil (Carter, 2004). In particular, there is a higher risk of compaction damage if the machinery used has not been adapted to the site and local conditions (Rücknagel et al., 2012; Koch et al., 2008). Compaction processes mainly affect parameters such as dry bulk density, aggregate stability, pore size distribution, infiltration rate and water conservation (FAO, 1993). This causes a deterioration in nutrient uptake and plant growth, while surface run-off increases (e.g. Paglai and Jones, 2002; Voorhees et al. 1986).

When investigating compaction effects in agricultural soils, conventional soil mechanical methods such as soil compression tests make it possible to map the compaction process and identify volumetric soil deformation for different initial soil structures. This yields indirect information about functional properties of the internal structure, such as the stress-strain relationship and aggregate density/bulk density ratio (Rücknagel et al., 2007). Typically, there is a lack of direct information about changes to geometric properties and morphologies of the void system. With this in mind, in recent decades non-destructive imaging methods, such as X-ray computed tomography (X-ray CT), have been increasingly used to successfully answer questions about soil physical properties (e.g. Keller et al., 2013; Schlüter et al., 2011, 2016a). Computed tomography not only detects the spatial distribution of pore geometries and maps their positions precisely, but also enables quantitative image analysis.

Only a few studies have dealt with the combined analysis of structural differences between individual conservation soil tillage systems and compaction effects in those soil tillage systems with the aid of computed tomography scans (e.g. Dal Ferro et al., 2014; Jarvis et al., 2017; Luo et al., 2010). None of these studies considered the strip tillage method. In addition, no links have been established between conventional soil mechanical methods and those involving computed tomography. Using a combination of soil mechanical and computed tomography methods, this study therefore focuses on the influence of the special, two-part soil structure present under strip tillage compared to mulch tillage and no tillage. Specifically, it aims to answer the following questions: (i) Does the strip tillage method create small-scale structural differences within and between the seed rows? (ii) Under strip tillage, how do dry bulk density and aggregate density change as stress increases compared to mulch tillage and no tillage? (iii) To what extent can morphometric parameters, based on X-ray CT, map soil compaction behaviour in strip tillage compared to mulch tillage and no tillage? (iv) Are there correlations between the parameters measured using conventional methods and those measured with X-ray CT? (v) And what implications do the results have for agricultural land use? Overall, this study aims to explore to evaluating the role of the different soil tillage methods in the compaction process.

2. Materials and methods

2.1. Trial site

Soil sampling was performed at the strip tillage experiment set up by the International Crop Production Centre in Bernburg-Strenzfeld (Germany, federal state Saxony-Anhalt, 11° 41′ E, 51° 50′ N; 80 m above sea level) in 2012. The average annual temperature is 9.7 °C and average annual precipitation is 511 mm. The soil type is a chernozem (FAO, 1998). The texture of the top soil (0–30 cm) contains 60 g kg^{-1} sand, 740 g kg^{-1} silt and 200 g kg^{-1} clay, constituting a silt loam (USDA, 1997). The total organic carbon content in the top soil is equal to 1.65 g kg^{-1} and the pH value is 6.8.

2.2 Experimental procedure

The field experiment is organized as a completely randomised block design including four blocks each with the treatments strip tillage, mulch tillage and no tillage. Each individual trial plot measures 18x50 m. Row spacing in the strip tillage treatment is 50 cm; the tilled strips measure 15–20 cm across and are ploughed to a depth of 20–25 cm. For strip tillage, there was no soil tillage between seed rows. Because of this differentiation in the strip tillage treatment, spatially separate samples were taken from within (strip tillage WS) and between (strip tillage BS) seed rows. These were considered as independent treatments for the rest of the experimental procedure and during evaluation. In the mulch tillage treatment, soil was tilled with cultivator to a depth of 15–20 cm, while the no tillage treatment was not tilled.

For the soil physical investigations, undisturbed soil samples (250 cm^3, height=6 cm) were taken in the years 2014 and 2015 in three replications per tillage treatment and field block from soil depths 2–8 cm (n=48) and 12–18 cm (n=48). In addition, 12 soil core samples (n=48) were taken from the same blocks used in the tillage treatments depths in the year 2012 before the trial was set up, in order to determine the initial physical conditions. The soil conditions at sampling time were always the same for all three sampling years (close to field capacity corresponding to a matric potential of -6 kPa) and always took place in the crop winter wheat.

Two types of soil compression test were conducted in the study. Only one load step was applied to those soil samples which were used to determine aggregate density (AD) after the soil compression tests (one load step application). With respect to the soil mechanical investigations, for each of 8 different load steps (5, 10, 25, 50, 100, 200, 350 and 550 kPa) undisturbed soil samples (220 cm^3, height=2.8 cm) were taken at soil depth 12–18 cm from each tillage treatment per field block (5x4x8=160 samples). The soil samples used in the computed tomography investigations after the soil compression tests were subjected to 8 successive load steps (classical load application) (Bradford and Gupta, 1986). For the computed tomography investigations, an undisturbed soil sample (220 cm^3) were taken at soil depth 12–18 cm from each tillage treatment per field block (5x4=20). These samples were also subject to the same loads steps, which were however applied successively with CT scans in between.

2.3. Soil compression test

The soil samples (220 cm^3) were first slowly saturated by capillary action before being drained for at least seven days in a sandbox with a hanging water column at a matric potential of -6 kPa (Klute, 1986) and then weighed.

The stress-strain relationship was determined in drained conditions with the aid of fully automated oedometers and software (WINBOD32, Wille Geotechnik, APS Antriebs-, Prüf- und Steuertechnik GmbH, Göttingen-Rosdorf, Germany). Loads were applied uniaxially. Compaction was performed parallel (one load step application) or successively (classical load application) for the load steps 5, 10, 25, 50, 100, 200, 350 and 550 kPa, with a load time of 120 min and a relaxation time with 2 kPa of 15 min. Previous studies showed that increasing the load time did not result in significant settlement in similar soils (Rücknagel et al., 2007). The dial indicator of the oedometer registered settlement with an accuracy of 0.01 mm.

After the soil compression test, soil samples were dried at 105°C for at least 48 hours and then weighed, in order to determine dry bulk density (BD) (Blake and Hartge, 1986). Based on settlement compared to the initial height of the soil sample and BD at the beginning of the trial, it is possible to calculate the resulting BD (BD_{xi}).

The measured values of classical load application were plotted in a semi-logarithmic stress-BD_{xi} diagram and form the basis of determining mechanical pre-compression stress ($\sigma_{P\ BDxi}$). Casagrande's (1936) graphical method was used for this. The graphical method was conducted by several independent experimenters so as to minimise its subjectivity (Rücknagel et al., 2010).

2.4. General soil physical investigations

The soil samples with a volume of 250 cm³ were used to identify the K_s value (cm d^{-1}) using a stationary system (Klute and Dirksen, 1986) with a flow duration of 4 h.

To determine AD, the soil samples were carefully broken up after the one load step application and aggregates with a diameter of 8–10 mm were sieved out. In three repeated measures, aggregates were submerged in vegetable oil (100 % rapeseed oil) until no more air leakage was detected and then drained on paper. The volume of the aggregates was then determined by means of immersion weighing in a measuring cylinder filled with water on scales with a measurement accuracy of

1/100 g. At a water density of 1.0 g cm^{-3}, the weight corresponds to the aggregates' volume (Rücknagel et al., 2007). In parallel, the aggregates' water content was determined in two repeated measures by drying them at 105°C for at least 48 h and then weighing them. The volume and dry mass of the aggregates can be used to calculate AD, which was reduced subsequently by 3.5 vol% to account for a minimal oil film on the aggregates. A test measurement using differential weighing served to calculate this correction value for the amount of oil present on the aggregates. The ratio of aggregate density to dry bulk density (AD/BD ratio) can be used as a measure of density heterogeneity in aggregated arable soils (Rücknagel et al. 2007). A low (<1.05–1.10) AD/BD ratio is an indication of damaging soil compaction, whereas a high (1.15–>1.20) AD/BD ratio suggests a loose soil structure (Rücknagel et al., 2013).

2.5. Computed tomography and image processing

The soil samples (220 cm^3) from the classical load application were scanned using an industrial X-ray scanner (X-Tek XCT225, Nikon Metrology) with an energy of 150 kV and a beam current of 550 µA. A scan consists of 2480 projections with an exposure time of 1.41 s (2 frames per projection). The projections were recorded on a CCD detector panel with 2000x1750 diodes. A 0.1 mm copper filter was used to reduce beam hardening. The CT scans were reconstructed using the X-Tek CT Pro software package with a spatial resolution of 60 µm and an 8-bit greyscale resolution. The Java software ImageJ 1.50e (Rasband, 1997–2015) was used for image processing.

In the case of classical load application, each application of a load step was followed by a CT scan, meaning that each soil sample was scanned eight times (n=160).

To reduce the volume of data and to exclude artefacts at the edge of the sample, mainly cracks and compaction, first a region of interest (ROI) with a circular diameter (90 mm) in the middle of the reconstructed CT scan was used. Since the soil volume decreased vertically as a result of compaction the ROI was adjusted in the z direction. This involved using the position of easily indentifiable, small rocks at the upper and lower ends of the sample. Consequently, it was always possible to locate the same fixed soil region within the sample regardless of compaction status. The ROI contained the sample volume from which all subsequent calculations were derived.

The CT scans were filtered using the "Non-local Means Denoising" plugin (Buades et al., 2005) in order to reduce scatter and noise. Segmentation occured automatically using Otsu's (1979) thresholding method, in order to separate the image into pores (black) and the soil matrix (white).

Pore size distribution was calculated using the maximum inscribed sphere method with the ImageJ Plugin "BoneJ – Thickness" (Doube, 2010). For each slice of a CT scan, macroporosity (pore diameter >60 µm) (Dewry et al., 2008) was quantified as a ratio of the number of pore voxels to the total number of voxels within the ROI. Similarly to the conventional identification of mechanical precompression stress, a double logarithmic graph of macroporosity against compressive stress was plotted; this was used to determine mechanical precompression stress ($\sigma_{P\ MP}$). Pore connectivity was calculated as a value between 0 and 1 using the ImageJ analysis "Particle Analyzer" (Ferreira and Rasband, 2010–2012). The ImageJ plugin "BoneJ – Anisotropy" (Doube, 2010) was used to calculate the degree of anisotropy as a value between 0 and 1, where 0 reflected the minimum (completely isotropic) and 1 the maximum (plate-like).

2.6. Statistical analysis

Statistical analysis was performed using the statistics software R Studio (0.99.893, R Foundation for Statistical Computing).

For the variance analyses, all parameters were tested for normal distribution (Shapiro-Wilk test) and variance homogeneity (Levene's test). First from the dependent repetitions and then from the field repetitions, the arithmetic mean value was determined for BD, BD_{xi}, AD, macroporosity, pore connectivity and anisotropy for each soil depth and tillage treatment separately. For the non-normally distributed values for saturated hydraulic conductivity and precompression stress, the arithmetic mean was calculated from the logarithmized values. The mean macropore diameter was determined based on the weighted average from the pore size distribution.

For the soil physical parameters BD and K_s, a two-way analysis of variance was conducted with soil tillage and year as independent factors. A one-way analysis of variance was conducted for the soil mechanical and for the morphometric parameters between load steps for the respective tillage treatment and between the individual tillage treatments within a particular load step. Using Tukey's honest significant difference test, differences among group mean values were identified and considered to be significant at a significance level of $p \leq 0.05$.

Furthermore, regression analyses were conducted between the BD and K_s values for each tillage treatment, with differences in the slopes of the regression lines regarded as significant with a significance level of $p \leq 0.05$.

Correlations were performed between the BD_{xi}, the AD and the AD/BD ratio of the one load step application and the mean macropore diameter, macroporosity, connectivity and anisotropy of the classical load application.

3. Results

3.1. Soil physical condition

Dry bulk density

Before the strip tillage trial was set up in 2012, BD at soil depths 2–8 cm and 12–18 cm was 1.15 g cm^{-3} and 1.36 g cm^{-3} respectively, regardless of tillage treatment (Tab. 1). In 2014 and 2015, neither depth displayed any significant differences in BD between mulch tillage and strip tillage WS on the one hand and strip tillage BS and no tillage on the other. By contrast, at both depths and in both years, BD was significantly lower for mulch tillage and strip tillage WS compared to strip tillage BS and no tillage.

Since the beginning of the trial in the year 2012, there was a significant decline in BD for mulch tillage and strip tillage WS at soil depth 2–8 cm in the year 2014, and at a soil depth of 12–18 cm in the years 2014 and 2015. Strip tillage BS and no tillage displayed a significant increase in BD over time, which was more prominent at soil depth 2–8 cm than at 12–18 cm.

Saturated hydraulic conductivity

In the year 2012, the K_s values at soil depths 2–8 cm and 12–18 cm were 111.3 cm d^{-1} and 26.7 cm d^{-1} respectively, regardless of tillage treatment (Tab. 1). In the years 2014 and 2015, differences in the K_s value were observed between tillage treatments at a soil depth of 2–8 cm. Because of high standard deviations these differences were only significant in the year 2015. In this respect, strip tillage WS had a significantly higher K_s value than no tillage. Mulch tillage and strip tillage BS did not differ significantly from strip tillage WS or from no tillage. At a soil depth of 12–18 cm, in 2014 there were no significant differences for mulch tillage and strip tillage WS on the one hand and strip tillage BS and no tillage on the other. Conversely, mulch tillage and strip tillage WS differed from strip tillage BS and no tillage in that they displayed significantly higher K_s values. In the year 2015, at 12–18 cm mulch tillage had a significantly higher K_s value than no tillage, while strip tillage WS and strip tillage BS did not differ significantly from mulch tillage and no tillage.

In the years 2014 and 2015, the K_s values at 12–18 cm were significantly higher than in 2012 for all tillage variants, with the exception of no tillage and strip tillage BS in 2014.

Relationship between dry bulk density and saturated hydraulic conductivity

The regression lines of the logarithmized K_s values with BD displayed negative linear relationships for all tillage treatments (Fig. 1). This means that as BD increased the K_s value decreased and vice versa. At BD >0.70, the coefficient of determination (r^2) was significant for the mulch tillage, strip tillage WS and no tillage treatments. The slope of the regression lines was significantly higher for strip tillage WS compared to strip tillage BS and no tillage.

3.2. Soil compression test with one stress application

Dry bulk density

In terms of BD_{xi}, the load steps 5 and 10 kPa resulted in no significant differences between mulch tillage and strip tillage WS or strip tillage BS and no tillage (Tab. 2). By contrast, mulch tillage and strip tillage WS displayed significantly lower BD_{xi} values than strip tillage BS and no tillage. Within the load steps 25 and 50 kPa, there was no significant difference between strip tillage BS and no tillage. Both did however display significantly higher BD_{xi} compared to mulch tillage. At the 350 kPa load step, there was no significant difference between mulch tillage and strip tillage WS. However, both displayed significantly lower BD_{xi} compared to strip tillage BS. In addition, mulch tillage had significantly lower BD_{xi} than no tillage. At the beginning of stress application, there was a maximum difference in dry bulk density between the treatments of 0.29 g cm^{-3}, which decreased to a maximum of 0.11 g cm^{-3} by the end of stress application. Overall, BD_{xi} increased by approximately 0.40 g cm^{-3} under mulch tillage and strip tillage WS, while the higher initial values meant that BD_{xi} only increased by around 0.25 g cm^{-3} in the strip tillage BS and no tillage treatments.

Aggregate density

Significant differences in AD between the tillage treatments were only seen for the 5 kPa load step (Tab. 2). There were no significant differences in AD between mulch tillage and strip tillage WS on the one hand or strip tillage BS and no tillage on the other. Strip tillage BS displayed significantly higher AD than strip tillage WS and mulch tillage. No tillage displayed significantly higher AD than strip tillage WS. At the beginning of stress application, there was a maximum difference in aggregate density between the treatments of 0.13 g cm^{-3}, although during the further course of stress application this resulted in similar final values of around 1.65 g cm^{-3}. Overall, AD increased under mulch tillage and strip tillage WS by around 0.20 g cm^{-3}, while the higher initial values meant that the AD only increased by around 0.05 g cm^{-3} in the strip tillage BS and no tillage treatments.

AD/BD ratio

Throughout the entire course of stress application, BD_{xi} was significantly lower at most load steps for mulch tillage (5–50, 350, 550 kPa) and strip tillage WS (5–25, 100 kPa) than the corresponding AD, while this only occurred in isolated cases in the strip tillage BS (10, 350 kPa) and no tillage treatments (5, 10, 100 kPa) (Fig. 2). For all tillage treatments, the compaction curves of BD_{xi} and AD converged as stress application increased, resulting in a decline of the AD/BD ratios (Tab. 2). At the 5 kPa load step, mulch tillage displayed a significantly higher AD/BD ratio than the other three tillage treatments. Within the 10 and 25 kPa load steps, there were no significant differences between strip tillage BS and no tillage, although they had a significantly lower AD/BD ratio than mulch tillage. As further load steps were applied, there were no further significant differences between tillage treatments, with the exception of the 350 kPa load step. Here, mulch tillage, strip tillage WS and strip tillage BS differed significantly from each other. Furthermore, no tillage displayed a significantly lower AD/BD ratio than mulch tillage. Overall, the AD/BD ratios for mulch tillage and strip tillage WS decreased by approximately 0.20 throughout the compaction process, while the AD/BD ratios for strip tillage BS and no tillage only decreased by around 0.15.

According to the classification of the AD/BD ratios outlined by Rücknagel et al. (2007), the soil structure under strip tillage WS changed from a blocky structure with open positioning and subangular aggregates with semi-open to open positioning to become a coherent mass with no visible aggregation. The soil in the strip tillage BS treatment initially displayed a blocky structure with semi-open to open positioning and subangular aggregates with semi-open positioning, and this also developed into a closed aggregate arrangement.

3.3. Conventional soil compression test

Dry bulk density and mechanical precompression stress

With regard to BD_{xi}, the load steps from 5–100 kPa yielded no significant differences between mulch tillage and strip tillage WS or between strip tillage BS and no tillage (Tab. 3, Fig. 3A). On the other hand, within the 5–25 kPa load steps mulch tillage and strip tillage WS displayed significantly lower BD_{xi} values than strip tillage BS and no tillage. At the 50 kPa load step, mulch tillage as well as strip tillage WS displayed significantly lower BD_{xi} values than strip tillage BS. In addition, mulch tillage displayed significantly higher BD_{xi} than no tillage. At the 100 kPa load step, mulch tillage displayed significantly lower BD_{xi} than strip tillage BS and no tillage. At the beginning of stress application, there was a maximum difference in dry bulk density between the tillage treatments of 0.29 g cm^{-3}; the rest of the compaction process resulted in similar density values of around 1.70 g cm^{-3}. Overall, as stress increased the BD_{xi} values under mulch tillage and strip tillage WS rose by approximately 0.45 g cm^{-3}, while the BD_{xi} values only increased by around 0.20 g cm^{-3} under strip tillage BS and no tillage.

The mechanical precompression stress values identified using the stress-BD_{xi} diagrams ($\sigma_{P\ BDxi}$) differed between the tillage systems. Strip tillage WS (log σ_P 1.58 = 38 kPa) displayed significantly lower mechanical precompression stress than strip tillage BS (log σ_P 2.15 = 141 kPa). Mulch tillage (log σ_P 1.67 = 46 kPa) and no tillage (log σ_P 2.05 = 112 kPa) did not differ significantly from each other or from strip tillage WS or strip tillage BS.

Morphometric parameters

Macropore structure characteristics of different tillage treatments are depicted for an individual sample from mulch tillage (Fig. 4) and no tillage (Fig. 5) at all 8 load steps and the following results are only true for pore sizes larger than 60 µm. The application of higher load steps resulted in only minor visual changes to the macropore space due to the higher initial density under no tillage. By contrast, under mulch tillage many macropores but also aggregates can be seen at the beginning of stress application. When the applied stress reached 50–100 kPa, the CT scans show that most macropores had already been reduced in size under mulch tillage. Overall, increased stress application resulted in a progressive homogenisation of the soil structure in both tillage treatments.

The reduction in the mean macropore size as stress increased was only significant under strip tillage WS (Tab. 3, Fig. 3B). The differences between the tillage treatments at the individual load steps were not significant. Apparently, there is a balance between bigger macropores merely being reduced within the visible range and smaller macropores being compacted beyond the image resolution limit and therefore excluded from averaging. Throughout the course of stress application, strip tillage BS and no tillage tended to display higher mean macropore sizes than mulch tillage and strip tillage WS. At the 550 kPa load step, all treatments displayed similar average final pore sizes around 0.55 mm.

The increase in compressive stress resulted in a decline in macroporosity and connectivity irrespective of tillage treatment, although this was only significant under mulch tillage and strip tillage WS (Tab. 3, Fig. 3C, 3D). For the load steps 5–25 kPa, there were significant differences in macroporosity and connectivity between the tillage treatments. At lower load steps, the pairs mulch tillage and strip tillage WS and no tillage and strip tillage BS differed significantly from each other with regard to macroporosity and connectivity, but hardly at all among each other. At the highest load steps, almost the entire void volume had been reduced and the tillage treatments displayed similar macroporosity and connectivity values.

The mechanical precompression stress values identified using the double logarithmic stress-macroporosity diagrams ($\sigma_{P\,MP}$) differed between the tillage systems (Tab. 3). There were no significant differences between mulch tillage (log σ_P 1.86 = 80 kPa) and strip tillage WS (log σ_P 1.69 = 50 kPa), while both displayed significantly lower mechanical precompression stress values compared to no tillage (log σ_P 2.39 = 270 kPa). Strip tillage BS (log σ_P 2.08 = 150 kPa) did not differ significantly from the other tillage treatments.

Increasing the stress application resulted in an change from isotropic to anisotropic conditions, regardless of the tillage treatment. Due to the broad distribution of values, the increase in anisotropy was only significant for mulch tillage and strip tillage WS at the load steps 350 and 550 kPa (Tab. 3, Fig. 3E). No significant differences were observed between tillage treatments.

3.4. Relationship between morphometric and soil mechanical parameters

Correlations were performed for all parameters of the one load step application with those of the classical load application (Fig. 6). The correlation coefficients determined in the context of the BD_{xi} were low and not significant for the mean macropore diameters (Fig. 6A). By contrast, the relationship between BD_{xi} and macroporosity (Fig. 6B), connectivity (Fig. 6C) and anisotropy (Fig. 6D) was significant and highly significant. As the BD increased, the volume fraction and connectivity of the macropores decreased while anisotropy increased.

The correlations identified with the AD (Fig. 6E, 6F, 6G, 6H) and AD/BD ratio (Fig. 6I, 6J, 6K, 6L) reflected the results just mentioned to a somewhat lesser extent.

4. Discussion

4.1. Soil physical condition

Overall, there were intact soil structures for all tillage treatments, depths and years where BD values were always lower than a site-specific, root-limiting BD of 1.55 g cm^{-3} (Kaufmann et al., 2010) and K_s values were higher than 10 cm d^{-1} (Werner and Paul, 1999).

The tillage treatments created different soil physical conditions. On the one hand strip tillage WS and mulch tillage, and on the other strip tillage BS and no tillage, each displayed very similar soil structural properties.

Strip tillage WS and mulch tillage displayed significantly lower BD compared to strip tillage BS and no tillage. This is due to the fact that the former had been loosened by soil tillage, while the latter were left untilled, with natural settlement as well as soil compaction occurring as a result of driving over the ground with agricultural machinery at the time of soil tillage and harvesting. This result is in line with those of other studies (e.g. Hubbard et al., 1994; Kay and Van den Bygaart, 2002). As time passed from 2014 to 2015, BD remained at a similar level at the depths sampled under strip tillage WS and mulch tillage, as the annual soil tillage counteracted the above-mentioned processes.

Overall, previous studies have shown contradictory results with respect to the K_s value for various tillage systems. Benjamin (1993) for example found that untreated variants promoted infiltration as a result of increased macroporosity. By contrast, some studies found that no tillage and other conservation-oriented soil tillage methods displayed lower K_s values compared to conventional soil tillage due to low macroporosity (e.g. Lindstrom and Onstad, 1984; Rücknagel et al., 2017). Other studies showed that there were no differences with respect to K_s values between untilled and conventionally tilled soils (Tollner et al., 1984; Culley et al., 1987). In this paper, strip tillage WS and mulch tillage displayed higher K_s values compared to strip tillage BS and no tillage, as the loosening soil tillage resulted in an increase in coarse interaggregate pores, which due to their higher flow cross section contributed to an increased saturated conductivity. At 12–18 cm soil depth, a significant increase in the K_s value was observed between 2012 and 2015 for mulch tillage, strip tillage WS and strip tillage BS, despite a slight increase in BD under strip tillage BS. This may have been caused by an increased earthworm population. At the same trial site, the earthworm population was recorded for the strip tillage WS and strip tillage BS variants in the spring of 2015. Here strip tillage WS (17.3 g m^{-2}; 68 individuals m^{-2}) was shown to have significantly lower earthworm abundance and biomass compared to strip tillage BS (36.7 g m^{-2}; 152 individuals m^{-2}) (Koblenz et al., 2016). Still, the spatial distance between strip tillage WS and BS is shorter than the size of the habittat of individual earthworms, which should be considered in the interpretation. The earthworms feel more comfortable in the more compacted BS region with increased moisture and cover with plant residues but may feed and move trough the less compacted WS region. Kay and Van den Bygaart (2002) also concluded that an increase in the number of biopores under no tillage was due to the earthworm population, which was able to develop well because of the high availability of food in the form of remaining dead plant matter and a lack of annual destruction. In the present study, however, these positive biological effects were only achieved in the strip tillage BS treatment.

It was thus possible to show that strip tillage combines, on a small scale, the soil physical properties of mulch tillage, as a deeper, non-turning form of primary tillage, and those of no tillage.

4.2. Soil compression tests

The soil structures which differed from each other on a small scale also reacted to mechanical loads in different ways. The loosened rows under strip tillage WS displayed mostly unstable secondary pores (cracks, irregular voids from loosening >60 µm). These were largely destroyed up to a load of approximately 100 kPa. At the same time, the annual soil tillage performed for strip tillage WS destroyed the structure and structural formation began again. This resulted in aggregates which were more porous and thus looser in their density. On the other hand, the lack of soil tillage in the strip tillage BS treatment guaranteed an undisturbed structural framework. The aggregates were not mechanically altered, and were further strengthened by mechanical loads from driving over the ground. This resulted in higher mechanical precompression stress ($\sigma_{P\ BDxi}$) compared to soil stress due to a high number of contact points between the aggregates and primary particles.

While the stress-BD_{xi} curves showed a standard path of a recompression and virgin compression line and mechanical precompression stress (Lebert and Horn, 1991), the behaviour was not observed in the stress-AD curves. The AD values of the different tillage treatments only increased to a limited extent during the compaction process, making it impossible to determine the mechanical precompression stress values from the stress-AD functions. It is possible that the highest load step of 550 kPa was still too low to obtain clear stress-AD curves, and thus mechanical precompression stress values, for the aggregates at this site. It would therefore make sense to select higher load steps. On the other hand, it could be that it is simply not possible to determine mechanical precompression stress from the stress-AD curves, since the aggregates do not display a standard compression curve, as is shown in Rücknagel et al. (2017). Overall, it can be stated that the soil compression mainly occurred because of compaction of interaggregate pores, which were not considered when measuring aggregate density.

At the beginning of stress application, there were isotropic initial structures regardless of tillage treatment, and no significant differences in anisotropy were identified between the tillage treatments during the entire stress application process. Up to the 200 kPa load step, strip tillage BS and no tillage tended to display not only higher mean pore diameters but also slightly higher anisotropies than strip tillage WS and mulch tillage. One reason for this could be the dominance of plant roots and biopores of macrofauna and their stable presence in untilled soils (Luo et al., 2010). Drees et al. (1994) also found higher mean pore diameters under no tillage than in conventionally tilled soils. Furthermore, vertically oriented pores are less susceptible to compaction than those aligned horizontally (Hartge and Bohne, 1983). In the case of uniaxial compaction, therefore, it can be assumed that horizontal pores were compacted first and only the vertical pores contributed to anisotropy. At the highest load steps, all tillage treatments displayed a sudden rise in anisotropy. This was also observed visually using the CT cross section, because by the end of stress application only isolated, irregularly distributed biopores remained.

The morphometric parameters macropore size, macroporosity and pore connectivity affect each other. One parameter which depends on pore size is connectivity (Jarvis et al., 2017). Generally speaking, the smaller the pores, the higher their connectivity (Vogel and Roth, 1998). Macroporosity also plays a role here. The higher the volume fraction of macropores, the higher the likelihood that macropores will be connected and form larger network (Luo et al., 2010). In the present study, no tillage displayed a few large, isolated macropores which resulted in a large pore radius, low macroporosity and low connectivity. At the same time, no tillage lacked the multitude of interaggregate pores smaller than the image resolution which, in the mulch tillage treatment, reduced the mean pore diameter and at the same time ensured higher macroporosity and connectivity. In the untilled treatments, the slightly higher mean macropore sizes did not coincide with a higher macroporosity. Pagliai (1988), who also worked with quantitative image analysis, includes a classification of macroporosity for pores >50 µm. According to this classification, mulch tillage and strip tillage WS were moderately porous at the beginning of stress application and strip tillage BS and no tillage were highly compacted. Furthermore, Pagliai (1988) describes macroporosity of 10 %, while Reynolds et al. (2009) uses quantitative image analysis to identify macroporosity of 4 %, as the lower limit for an intact soil structure, which is not achieved for strip tillage BS and no tillage. Similar results concerning macroporosity with conservation-oriented methods compared to conventional soil tillage are reported by Bullock et al. (1985) and Gantzer and Anderson (2002). In studies by Jarvis et al. (2017) and Dal Ferro et al. (2014), comparable experimental conditions also yielded similar values for the morphometric parameters from the quantitative image analysis of computed tomography scans to those at the Bernburg site.

In addition to the conventional procedure using stress-BD_{xi} diagrams, mechanical precompression stress values were also determined for the tillage treatments based on the double logarithmic stress-macroporosity diagrams ($\sigma_{P\ MP}$) from the CT investigations. These showed good agreement with the values identified from the stress-BD_{xi} diagrams ($\sigma_{P\ BDxi}$). Besides the general suitability of $\sigma_{P\ MP}$, the diagrams' double logarithmized representation means it is also necessary to examine the extent to which there may be visual distortion with regard to the strongest curvature of the stress-macroporosity curves, which is one of the bases of Casagrande's (1936) graphical method. Overall, it can be noted that for all treatments there seems to be a critical stress value at around 100 kPa where macroporosity and connectivity reached an irreducible minimum and anisotropy increased considerably, yet with a rather high variability due to the variable morphology of the remaining few macropores, as was evident from the CT cross sections. A similar stress value for soil structure deformation was reported for compaction during centrifugation (Schlüter et al. 2016a). This critical stress value is reflected well by the mechanical precompression stress values of the individual tillage treatments.

In the present study, the correlations of the pore properties macroporosity and connectivity with BD indicated a non-linear relationship, whereas the mean macropore diameter displayed a linear relationship with BD. Schlüter and Vogel (2016b) observed linear behaviour when comparing porosity with mean pore size, and non-linear behaviour when comparing porosity with connectivity. At a critical porosity value of 10–12 %, the collapse of the well-connected network of pores then led to a large number of uniform, isolated pores. This abrupt transition resulted from the regular packing of an artificially produced soil (texture: silt loam) consisting of aggregates of equal size. In the present study, the decline in macroporosity and connectivity as BD increased was somewhat gradual, since the extraction of undisturbed soil samples preserved the natural heterogeneous structure and its irregular network of pores.

It should be pointed out that the present study only involved uniaxial compaction. In practice, driving over the field with agricultural machinery also subjects the soil to dynamic loads. In addition, the spatial propagation of pressure is three-dimensional. Nevertheless, the results identified in the present study can be transferred to the field level, because the greatest principal stress acts in the direction of the maximum force applied, which is also vertical in naturally layered soils (Horn and Peth, 2011).

5. Conclusions

The tillage treatments displayed clear differences in terms of initial structure and compaction behaviour. In addition to higher mechanical precompression stress values under strip tillage BS and no tillage, these also showed higher BD_{xi} and AD throughout almost the entire load range compared to strip tillage WS and mulch tillage. The CT scans and the morphometric parameters also confirmed the mechanically more stable soil structure under strip tillage BS and no tillage, with higher mean macropore diameters and lower macroporosity and connectivity values, compared to strip tillage WS and mulch tillage. At the same time, it was shown for all tillage treatments that stress application resulted in a decrease in mean macropore diameter, macroporosity and connectivity, and an increase in anisotropy.

Strip tillage combined the conventional advantages of no tillage with those of deeper, non-turning primary tillage, because strip tillage WS and mulch tillage as well as strip tillage BS and no tillage each displayed very similar soil structural properties. Strip tillage thus offers farmers an advantageous soil structure which is capable of sufficiently withstanding mechanical stresses in the areas between seed rows which are driven over, and at the same time allows optimum conditions for plant growth.

It should also be noted that the classically determined soil mechanical parameters are closely related to the computed tomography parameters, with the latter usefully complementing the former. The morphometric parameters thus provide valuable information about the influence of soil tillage on a microscopic level, improving our understanding of the effects of tillage methods on soil functions on the whole.

Acknowledgments

The authors would like to thank the “Internationales DLG-Pflanzenbauzentrum Bernburg-Strenzfeld” for allowing them to take the soil samples at the Bernburg site. We gratefully acknowledge the expert technical assistance and guidance of J. M. Köhne and are grateful to V. Hentschel and F. Hickmann for their support in the field and laboratory work.

References

Benjamin, J.G., 1993. Tillage effects on near-surface soil hydraulic properties. Soil Till. Res. 26 (4), 277–288.

Blake, G. R., Hartge, K. H., 1986. Bulk Density. In: Klute, A. (Ed.), Methods of soil analysis. Part 1: Physical and mineralogical methods, Second Edition Madison,Wisconsin, USA, pp. 363–382.

Bradford, J.M., Gupta, S.C., 1986. Compressibility. In: Klute, A. (Ed.), Methods of soil analysis. Part 1: Physical and mineralogical methods, Second Edition Madison,Wisconsin, USA, pp. 479–492.

Buades, A., Coll, B., Morel, J.M., 2005. A Review of Image Denoising Algorithms, with a New One. Multiscale Model. Simul. 4(2), 490–530.

Bullock, P., Newman, A.C.D., Thomasson, A.J., 1985. Porosity aspects of the regeneration of soil structure after compaction. Soil Till. Res. 5(4), 325–341.

Carter, M.R., 2004. Researching structural complexity in agricultural soils. Soil Till. Res. 79, 1–6.

Casagrande, A. 1936. The determination of the pre-consolidation load and its practical significance. Proceedings of the International Conference on Soil Mechanics and Foundation Engineering, vol. III, pp. 60–64. Harvard University, Cambridge.

Culley, J.L.B., Larson, W.E., Randall, G.W., 1987. Physical properties of a Typic Haplaquoll under conventional and no-tillage. Soil Sci. Soc. Am. J. 51, 1587–1593.

Dal Ferro, N., Sartori, L., Simonetti, G., Berti, A., Morari, F., 2014. Soil macro- and microstructure as affected by different tillage systems and their effects on maize root growth. Soil Till. Res. 140, 55–65.

Dewry, J. J., Cameron, K. C., Buchan, G. D., 2008. Pasture yield and soil physical property responses to soil compaction from treading and grazing – a review. Aust. J. Soil Res. 46, 237–256.

Doube, M., Klosowski, M.M., Arganda-Carreras, I., Cordelieres, F., Dougherty, R.P., Jackson, J., Schmid, B., Hutchinson, J.R., Shefelbine, S.J., 2010. BoneJ: free and extensible bone image analysis in ImageJ. Bone 47, 1076–9.

Drees, T., Karathanasis, A.D., Wilding, L.B., Belvins, R.L., 1994. Micromorphological characteristic of long-term no-tillage and conventionally tilled soils. Soil Sci. Soc. Am. J. 58, 508–517.

FAO, 1993. Soil tillage in Africa: needs and challenges. FAO Soils Bulletin, 69. FAO, Rome, Italy.

FAO, 1998. World Reference Base for Soil Resources. ISSS–ISRIC–FAO. World Soil Resources Report No. 84. Rome.

Ferreira, T., Rasband, W.S., 2010-2012. “ImageJ User Guide — IJ 1.46”, imagej.nih.gov/ij/docs/guide/

Gajri, P.R., Gill, K.S., Singh, R., Gill, B.S., 1999. Effect of pre-planting tillage on crop yields and weed biomass in a rice-wheat system on a sandy loam soil in Punjab, Soil Till. Res. 52, 83–89.

Gantzer, C.J., S.H. Anderson. 2002. Computed tomographic measurement of macroporosity in chisel-disk and no-tillage seedbeds. Soil Till. Res. 64, 101–111.

Hartge, K.H., Bohne, H., 1983. Effect of pore geometry on compressibility of soil and development of rye seedlings. Z. f. Kulturtechnik und Flurbereinigung 24, 5–10.

Horn, R., Peth, S., 2011. Stress–Strain Relationships: A Possibility to Quantify Soil Strength Defined as the Precompression Stress. In: Encyclopedia of Agrophysics (Eds J. Gliński, J. Horabik and J. Lipiec). Springer Press, Dordrecht-Heidelberg- London-New York.

Hubbard, R.K., Hargrove, W.L., Lowrande, R.R., Williams, R.G., Mullinix, B.G., 1994. Physical properties of a clayey coastal plain soil as affected by tillage. J. Soil Water Conserv. 49, 276–283.

Jarvis, N., Larsbo, M., Koetsel, J., 2017. Connectivity and percolation of structural pore networks in a cultivated silt loam soil quantified by X-ray tomography. Geoderma, 287, 71–79.

Kaufmann, M., Tobias, S., Schulin, R., 2010. Comparison of critical limits for crop plant growth based on different indicators for the state of soil compaction. J. Plant Nutr. Soil Sci. 173, 573–583.

Kay, B.D., Van den Bygaart, A.J., 2002. Conservation tillage and depth stratification of porosity and soil organic matter. Soil Till. Res., 66, 107–118.

Keller, T., Lamand, M., Peth, S., Berli, M., Delenne, J.-Y., Baumgarten, W., Rabbel, W., Radja, F., Rajchenbach, J., Selvadurai, A., Or, D., 2013. An interdisciplinary approach towards improved understanding of soil deformation during compaction. Soil Till. Res. 128, 61–80.

Klute, A., 1986. Water Retention: Laboratory Methods. In: Klute, A. (Ed.), Methods of soil analysis. Part 1: Physical and mineralogical methods, Second Edition Madison,Wisconsin, USA, pp. 635–662.

Klute, A., Dirksen, C., 1986. Hydraulic Conductivity and Diffusivity: Laboratory Methods. In: Klute, A. (Ed.), Methods of soil analysis. Part 1: Physical and mineralogical methods, Second Edition Madison,Wisconsin, USA, pp. 687–734.

Koblenz, B., Umann, M., Wensch-Dorendorf, M., Rücknagel, J., Christen, O., 2016. Impact of different tillage systems in root growth and earthworm population in maize. Proceedings of the European Society of Agronomy Conference 14, pp. 49–50. Edinburgh, Scotland.

Koch, H.J., Heuer, H., Tomanova, O., Märländer, B., 2008. Cumulative effect of annually repeated passes of heavy agricultural machinery on soil structural properties and sugar beet yield under two tillage systems. Soil Till. Res. 101, 69–77.

Lal, R. 1983. No-tillage farming: Soil and water conservation and management in the humid and sub-humid tropics. IITA Monograph No. 2, Ibadan, Nigeria.

Lebert, M., Horn, R., 1991. A method to predict the mechanical strength of agricultural soils. Soil & Till. Res. 19, 275–286.

Licht, M. A., Al-Kaisi, M., 2005b. Strip-tillage effect on seedbed soil temperature and other soil physical properties. Soil Till. Res. 80(1), 233–249.

Lindstrom, M.J., Onstad, C. A., 1984. Influence of tillage systems on soil physical parameters and infiltration after planting. J. Soil Water Conserv. 39, 149–152.

Luo, L., Lin, H., Li, S., 2010. Quantification of 3-D soil macropore networks in different soil types and land uses using computed tomography. J. of Hydrol. 393(1), 53–64.

Nowatzki, J., Endres, G., DeJong-Hughes, J., Aakre, D., 2009. Strip tillage for Field Crop Production: Equipment, Production, Economics. North Dakota State University Extension Service.

Otsu, N., 1979. A Treshold Selection Method from Gray-Level Histograms. IEEE Trans. Syst. Man, Cybern. B, Cybern. Vol SMC-9, NO. 1, 62–66.

Pagliai, M., 1988. Soil porosity aspects. Intern. Agrophysics, 4: 215-232.

Paglai, M., Jones, R., 2002. Sustainable Land Management – Environmental Protection – A Soil Physical Approach. Advances in Geo Ecology, 35, Catena, Reiskirchen.

Rasband W.S., 1997–2015. ImageJ. Bethesda, Maryland, USA: U. S. National Institutes of Health; http://imagej.nih.gov/ij/

Reynolds, W.D., Drury, C.F., Tan, C.S., Fox, C.A., Yang, X.M., 2009. Use of indicators and pore volume-function characteristics to quantify soil physical quality. Geoderma 152, 252–263.

Rücknagel, J., Hofmann, B., Paul, R., Christen, O., Hülsbergen, K., 2007. Estimating precompression stress of structured soils on the basis of aggregate density and dry bulk density. Soil Till. Res. 92(1–2), 213–220.

Rücknagel, J., Brandhuber, R., Hofmann, B., Lebert, M., Marschall, K., Paul, R., Stock, O., Christen, O., 2010. Variance of mechanical precompression stress in graphic estimations using the Casagrande method and derived mathematical models. Soil Till. Res. 106, 165–170.

Rücknagel, J., Rücknagel, S., Christen, O., 2012. Impact on soil compaction of driving agricultural machinery over ground frozen near the surface. Cold Reg. Sci. Technol. 70, 113–116.

Rücknagel, J., Dumbeck, G., Harrach, T., Höhne, E., Christen, O., 2013. Visual structure assessment and mechanical soil properties of re-cultivated soils made up of loess. Soil Use Manag. 29, 271–278.

Rücknagel, J., Rademacher, A., Götze, P., Hofmann, B., Christen, O., 2017. Uniaxial compression behaviour and soil physical quality of topsoils under conventional and conservation tillage. Geoderma 286, 1–7.

Schlüter, S., Leuther, F, Vogler, S., Vogel, H.-J., 2016a. X-ray microtomography analysis of soil structure deformation caused by centrifugation. Solid Earth 7, 129–140.

Schlüter, S., Vogel, H.-J., 2016b. Analysis of Soil Structure Turnover with Garnet Particles and X-ray Microtomography. PLoS ONE 17, 1-17.

Schlüter, S., Weller, U., Vogel, H.-J., 2011. Soil structure development including seasonal dynamics in a long-term fertilization experiment. J. Plant Nutr. Soil Sci. 174, 395–403.

Tollner, E., Hargrove, W., Langdale, G., 1984. Influence of conventional and no-tillage practices on soil physical properties in the southern Piedmont. J. of Soil and Water Consv. 39(1), 73–76.

USDA, 1997. Keys to Soil Taxonomy by the Soil Survey Staff, Soil Conservation Service, U.S. Department of Agriculture (USDA), 7th ed. Pocahontas Press, Blacksburg, Virginia.

Vogel, H.J., Roth, K., 1998, A new approach for determining effective soil hydraulic functions, Europ. J. Soil Sci., 49, 547–556.

Voorhees, W.B., 1986. The effect of compaction on crop yield. Proc. Earthmoving Industry Conf., Paper No. 860729, Peoria, IL, 7 pp.

Werner, D., Paul, R., 1999. Kennzeichnung der Verdichtungsgefährdung landwirtschaftlich genutzter Böden. Wasser und Boden 51(12), 10–14.

757

Tab. 1: Bulk density (BD, g cm^{-3}) and saturated hydraulic conductivity (K_s, cm d^{-1}) at 2–8 and 12–18 cm depth for mulch tillage (MT), strip tillage within the seed row (STWS), strip tillage between seed rows (STBS) and no tillage (NT). Statistical significances ($p \leq 0.05$) are in lower-case letters (tillage system within year and depth) and upper-case letters (year within tillage system and depth).

Parameter	Depth (cm)	Year	Tillage system			
			MT	STWS	STBS	NT
BD (g cm^{-3})	2–8	2012	1.15 aB	1.15 aB	1.15 aA	1.15 aA
		2014	1.09 aA	1.06 aA	1.29 bB	1.28 bB
		2015	1.11 aAB	1.09 aAB	1.39 bC	1.43 bC
	12–18	2012	1.36 aB	1.36 aB	1.36 aA	1.36 aA
		2014	1.21 aA	1.17 aA	1.41 bAB	1.41 bAB
		2015	1.24 aA	1.22 aA	1.42 bB	1.45 bB
K_s (cm d^{-1})	2–8	2012	111.3 aA	111.3 aA	111.3 aA	111.3 aA
		2014	227.3 aA	255.0 aA	81.7 aA	109.8 aA
		2015	144.9 abA	295.0 bA	39.8 abA	30.4 aA
	12–18	2012	26.7 aA	26.7 aA	26.7 aA	26.7 aA
		2014	145.9 bB	158.2 bB	34.8 aAB	45.2 aA
		2015	147.5 bB	107.6 abB	81.7 abB	22.5 aA

Fig. 1: Regression between bulk density (BD, g cm^{-3}) and log K_s (cm d^{-1}) at 2–8 and 12–18 cm depth in the years 2012, 2014 and 2015 for mulch tillage (MT), strip tillage within the seed row (STWS), strip tillage between seed rows (STBS) and no tillage (NT) with formula (y = slope * x + intercept), coefficient of determination (r^2), p-value (≤0.05, significant) and different lower-case letters showing statistical significances between the slopes (p≤0.3, significant).

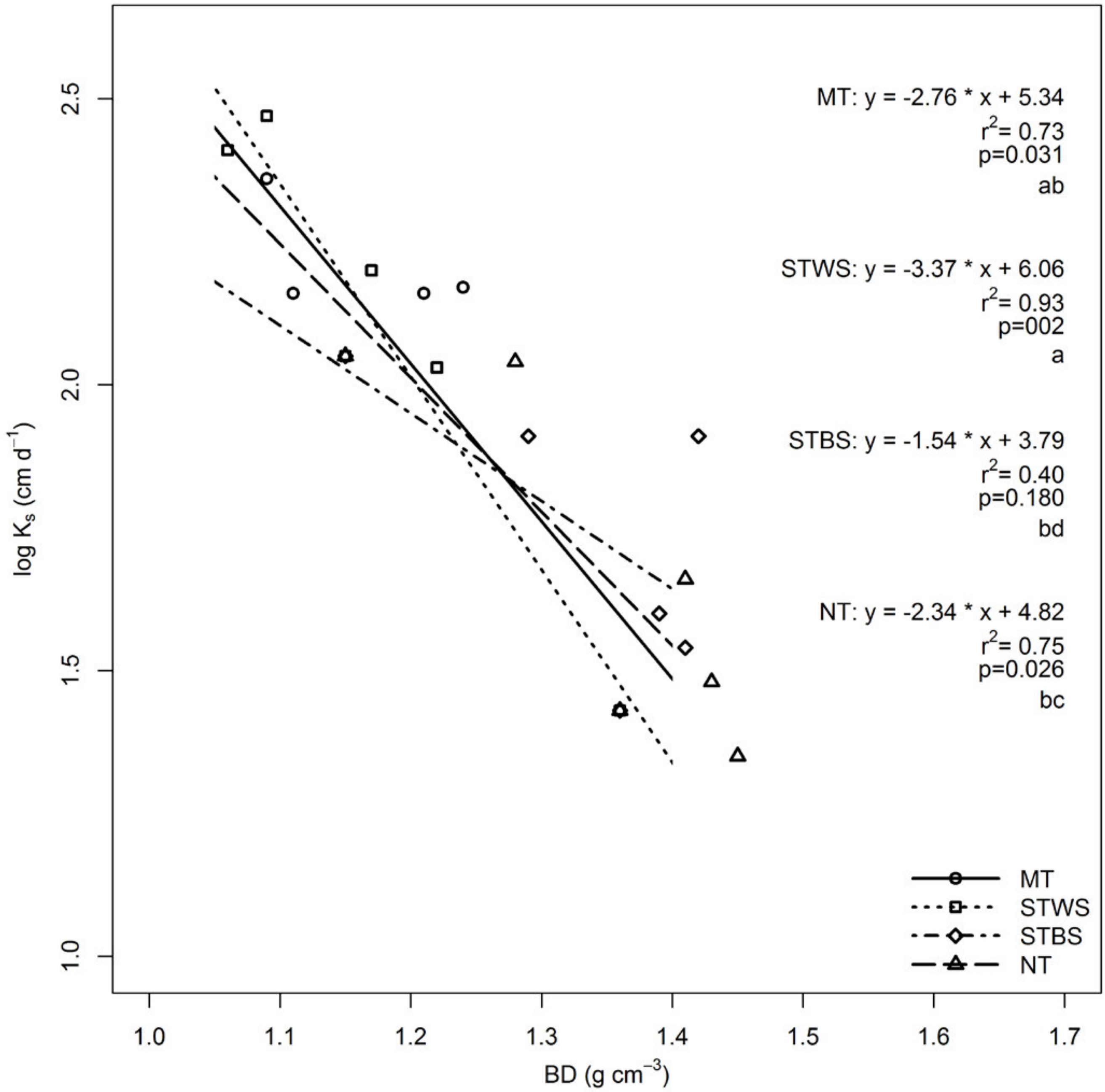

Tab. 2: Bulk density (BD_{xi}, g cm^{-3}), aggregate density (AD, g cm^{-3}) and AD/BD ratio (-) from one load step application per soil core at 12–18 cm depth for mulch tillage (MT), strip tillage within the seed row (STWS), strip tillage between seed rows (STBS) and no tillage (NT). Statistical significance ($p \leq 0.05$) is indicated by lower-case letters (load step within each tillage system) and upper-case letters (tillage system within each load step).

Parameter	Tillage system	Load step (kPa)							
		5	10	25	50	100	200	350	550
BD_{xi} (g cm^3)	MT	1.14 aA	1.20 abA	1.27 abA	1.31 abcA	1.44 abcA	1.47 acdA	1.49 cdA	1.57 dA
	STWS	1.21 aA	1.23 aA	1.30 abAB	1.38 abcAB	1.46 bcdA	1.49 bcdA	1.53 cdAB	1.61 dA
	STBS	1.43 aB	1.45 aB	1.46 abB	1.53 abB	1.55 bcA	1.59 cdA	1.65 deC	1.68 eA
	NT	1.40 aB	1.47 aB	1.45 abB	1.48 abAB	1.53 bcA	1.59 cdA	1.61 deBC	1.66 eA
AD (g cm^3)	MT	1.47 aAB	1.47 aA	1.51 abA	1.50 abA	1.51 abA	1.59 bcA	1.62 cA	1.66 cA
	STWS	1.45 aA	1.50 aA	1.48 aA	1.49 aA	1.56 abA	1.50 aA	1.58 abA	1.66 bA
	STBS	1.58 aC	1.59 aA	1.51 aA	1.59 aA	1.55 aA	1.57 aA	1.58 aA	1.63 aA
	NT	1.57 aBC	1.55 aA	1.53 aA	1.54 aA	1.60 aA	1.59 aA	1.58 aA	1.60 aA
AD/BD (-)	MT	1.31 aB	1.30 aB	1.21 abB	1.10 bA	1.08 bA	1.13 abA	1.09 bC	1.07 bA
	STWS	1.20 acA	1.22 aAB	1.14 abcAB	1.08 abcA	1.07 abcA	1.00 bA	1.03 bB	1.04 bcA
	STBS	1.11 aA	1.09 aA	1.03 abA	1.04 abA	1.00 abA	0.99 bA	0.95 bA	0.97 bA
	NT	1.12 bA	1.06 abA	1.06 abA	1.04 abcA	1.04 abcA	1.00 acA	0.98 acAB	0.96 cA

Tab. 3: Bulk density (BD_{xi}, g cm^{-3}), mean macropore diameter (mm), macroporosity (-), anisotropy (-), connectivity (-) and logarithmic precompression stress ($\log\sigma_P$) from classical load application at 12–18 cm depth for mulch tillage (MT), strip tillage within the seed row (STWS), strip tillage between seed rows (STBS) and no tillage (NT). Statistical significance ($p \leq 0.05$) is indicated by lower-case letters (load step within each tillage system) and upper-case letters (tillage system within each load step).

Parameter	Tillage system	Stress stage (kPa)								$\log \sigma_P$
		5	10	25	50	100	200	350	550	
BD_{xi} (g cm^3)	MT	1.23 bA	1.24 abA	1.3 acA	1.35 cA	1.42 dA	1.52 eA	1.61 fA	1.68 gA	1.67 AB
	STWS	1.25 aA	1.28 aA	1.34 abA	1.41 abAB	1.49 bcAB	1.58 cdA	1.66 deA	1.71 eA	1.58 A
	STBS	1.52 aB	1.53 aB	1.55 aB	1.57aC	1.59 aB	1.62 aA	1.64 aA	1.67 aA	2.15 B
	NT	1.45 aB	1.47 aB	1.49 abB	1.52 abBC	1.55 bcB	1.59 cdA	1.65 deA	1.70 eA	2.05 AB
Mean macropore diameter (mm)	MT	0.72 aA	0.72 aA	0.64 aA	0.64 aA	0.56 aA	0.47 aA	0.53 aA	0.55 aA	-
	STWS	0.94 aA	0.92 aA	0.88 aA	0.82 abA	0.65 abA	0.51 bA	0.51 bA	0.53 bA	-
	STBS	0.95 aA	1.12 aA	1.06 aA	1.13 aA	1.10 aA	0.90 aA	0.76 aA	0.64 aA	-
	NT	1.14 aA	1.21 aA	1.19 aA	1.16 aA	1.13 aA	0.83 aA	0.59 aA	0.48 aA	-
Macroporosity (-)	MT	0.12 aB	0.10 aC	0.08 abB	0.04 bcA	0.02 bcA	0.01 cA	0.01 cA	0.00 cA	1.86 A
	STWS	0.10 aB	0.09 aBC	0.06 abAB	0.03 bcA	0.02 bcA	0.01 cA	0.00 cA	0.00 cA	1.69 A
	STBS	0.02 aA	0.02 aA	0.02 aA	0.01 aA	0.01 aA	0.01 aA	0.01 aA	0.00 aA	2.08 AB
	NT	0.04 aA	0.04 aAB	0.03 aA	0.03 aA	0.02 aA	0.01 aA	0.01 aA	0.00 aA	2.39 B
Connectivity (-)	MT	0.80 aB	0.74 aC	0.67 aB	0.22 bA	0.08 bA	0.03 bA	0.03 bA	0.05 bA	-
	STWS	0.69 aB	0.60 aBC	0.39 abAB	0.17 bcA	0.07 cA	0.03 cA	0.06 cA	0.07 cA	-
	STBS	0.08 aA	0.09 aA	0.08 aA	0.08 aA	0.09 aA	0.07 aA	0.05 aA	0.06 aA	-
	NT	0.16 aA	0.14 aAB	0.08 aA	0.09 aA	0.06 aA	0.07 aA	0.06 aA	0.04 aA	-
Anisotropy (-)	MT	0.18 aA	0.18 aA	0.16 aA	0.17 aA	0.17 aA	0.25 aA	0.86 bA	0.88 bA	-
	STWS	0.22 aA	0.23 aA	0.25 aA	0.25 aA	0.20 aA	0.22 aA	0.83 bA	0.91 bA	-

STBS	0.27 aA	0.26 aA	0.26 aA	0.22 aA	0.44 aA	0.45 aA	0.40 aA	0.88 aA	-
NT	0.28 aA	0.29 aA	0.30 aA	0.24 aA	0.30 aA	0.30 aA	0.54 aA	0.77 aA	-

Fig. 2: Bulk density (BD_{xi}, g cm^{-3}) and aggregate density (AD, g cm^{-3}) at 12–18 cm depth from one load step application per soil core for mulch tillage (MT), strip tillage within the seed row (STWS), strip tillage between seed rows (STBS) and no tillage (NT). Error bars show standard deviation and different lower-case letters indicate statistical significance ($p \leq 0.05$) between BD_{xi} and AD for each load step.

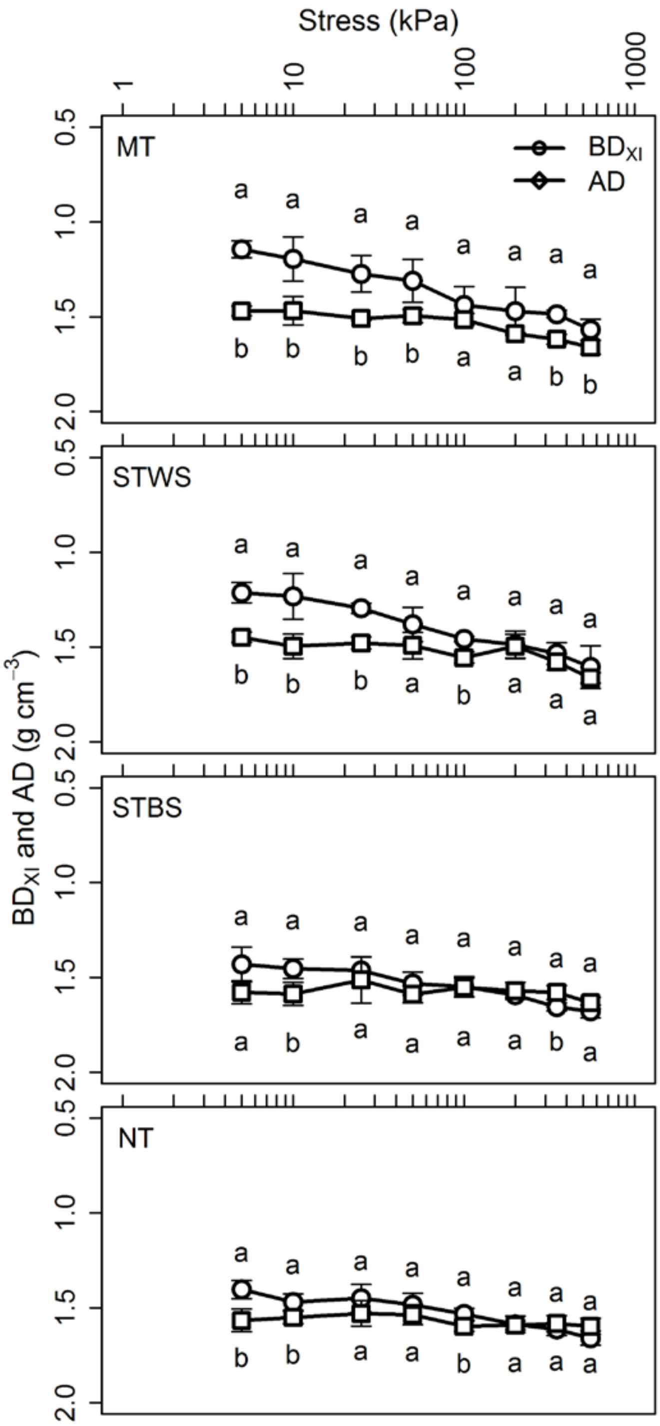

Fig. 3: (A) Bulk density (BD_{xi}, g cm^{-3}), (B) mean macropore diameter (mm), (C) macroporosity (-), (D) connectivity (-) and (E) anisotropy (-) at 12–18 depth from classical load application (kPa) for mulch tillage (MT), strip tillage within the seed row (STWS), strip tillage between seed rows (STBS) and no tillage (NT). Error bars show standard deviation.

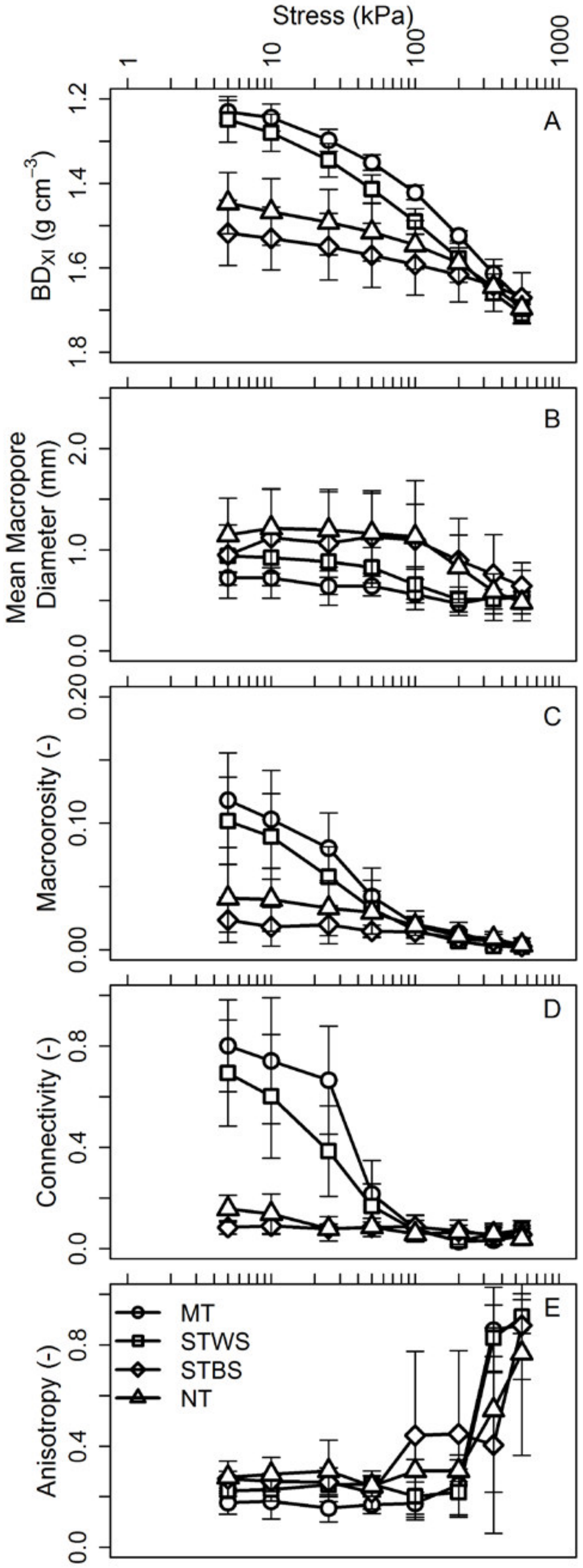

821 Fig. 4: CT cross section images from classical load application from 5 to 550 kPa load steps for mulch tillage (MT).

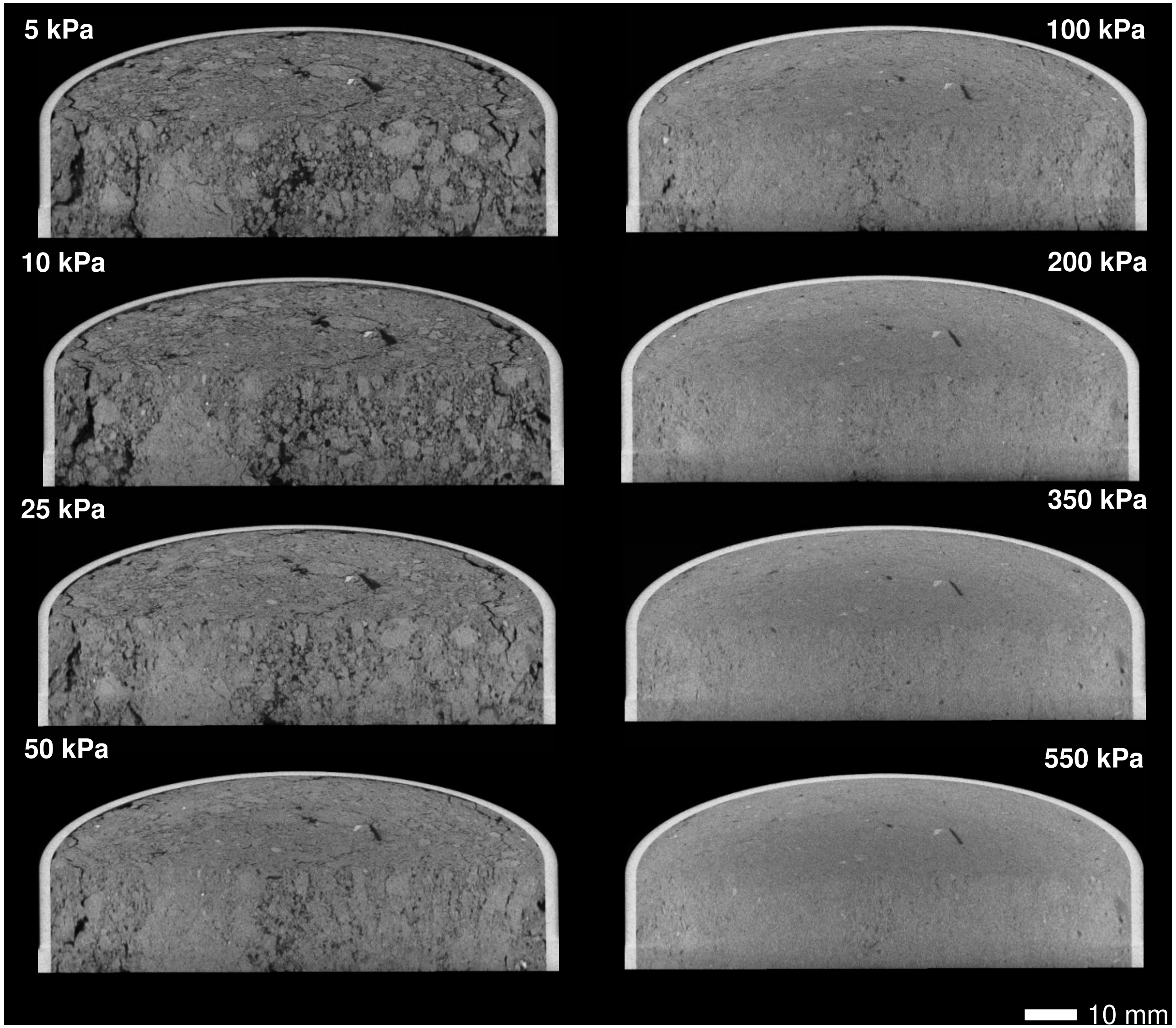

822

823 Fig. 5: CT cross section images from classical load application from 5 to 550 kPa load steps for no tillage (NT).

824 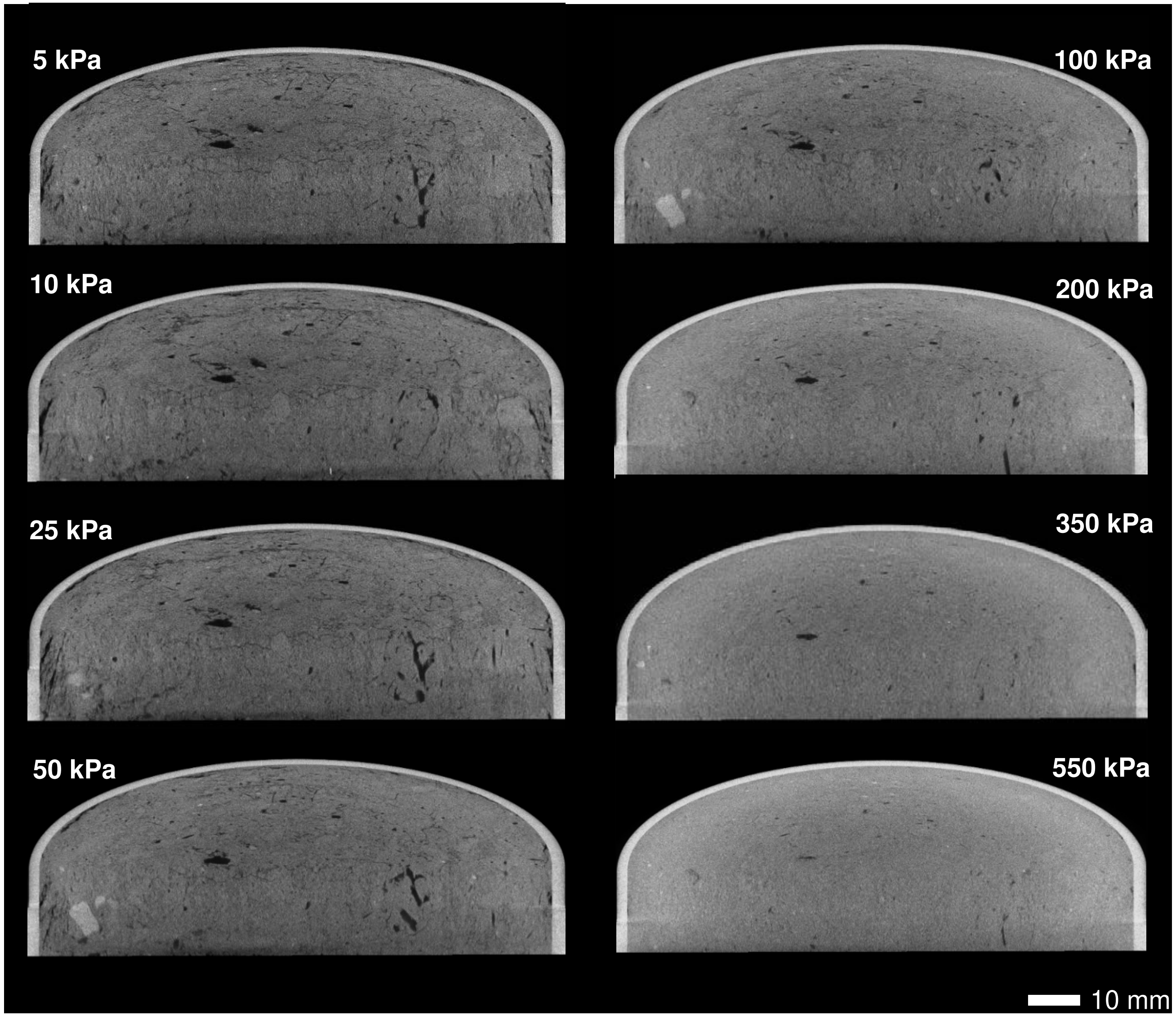

Fig. 6: Correlation between bulk density (BD_{xi}, g cm^{-3}), AD, AD/BD ratio of one load step application and mean macropore diameter (mm), macroporosity (-), connectivity (-), anisotropy (-) of classical load application at 12–18 cm depth for mulch tillage (MT), strip tillage within the seed row (STWS), strip tillage between seed rows (STBS) and no tillage (NT) with total correlation coefficients (r) and p-values (≤0.05, significant).